Available online at www.sciencedirect.com

SCIENCE DIRECT®

ELSEVIER

Synthetic Metals 152 (2005) 329–332

SYNTHETIC METALS

www.elsevier.com/locate/synmet

First principle study of the adsorption of atomic hydrogen on cluster-model surfaces

Yasuhito Ohta [a,b] and Koji Ohta [b*]

[a] *Japan Science and Technology Corporation*
[b] *Photonics Research Institute, AIST Kansai, Ikeda, Osaka 563-8577, Japan*

Abstract

The interactions of hydrogen with graphitic $C_{16}H_{10}$ and $B_8N_8H_{10}$ clusters are investigated by performing hybrid density functional electronic structure calculations. The B3LYP results are presented for both the H-$C_{16}H_{10}$ and H-$B_8N_8H_{10}$ clusters. For H-$C_{16}H_{10}$, significant structural relaxation of the $C_{16}H_{10}$ substrate is observed, while for H-$B_8N_8H_{10}$ the $B_8N_8H_{10}$ substrate is allowed to keep a planar structure at their optimized geometry. From the analyses of electron density and potential energy surface, the former interaction is shown to be chemisorption and the latter physisorption. The mechanism of hydrogen adsorption on the substrates is discussed using energetic diagram in the HOMO-LUMO region.

Keywords: Ab initio quantum chemical methods and calculations, Density functional calculations, Models of surface and interface chemistry and physics, Graphite and related compounds, Fuel storage devices

1. Introduction

The study of hydrogen adsorption on organic [1] or inorganic [2] materials has been of importance toward the technological application of hydrogen storage. In particular, carbon materials such as graphite and carbon nanotubes have been expected to be promising systems for efficient hydrogen storage because they can take diverse structural forms and those natural resources are abundant [1]. Recently, several researchers have theoretically studied hydrogen adsorption by applying semi-empirical [3-5] and first principle [6-8] approaches to the graphite-like cluster models. Jeloaica and Sidis have investigated the adsorption region of atomic hydrogen on a coronene-like graphite surface from the first principle calculations based on density-functional theory (DFT) [6]. Ferro et al. have explored stable sites of the adsorbed hydrogen on several graphite-like cluster models [7,8]. They have shown that the pyrene-like $C_{16}H_{10}$ cluster is efficient for reproducing the H-graphite interaction of more extended systems.

Besides above-mentioned carbon materials, boron nitride (BN) materials have also attracted considerable attention due to their peculiar characteristics [9-18]. The heat-resistance and chemical stability of graphite-like BN materials are generally superior to carbon materials. These characteristics of BN materials are expected to be important for realization of efficient hydrogen storage. In order to clarify the mechanism of the hydrogen adsorption on the BN materials, we focus our study on the use of the pyrene-like $B_8N_8H_{10}$ cluster model.

In the present study, we investigate the adsorption of atomic hydrogen on $C_{16}H_{10}$ and $B_8N_8H_{10}$ by performing first-principle electronic structure calculations. The structural properties of H-$B_8N_8H_{10}$ are compared with those of H-$C_{16}H_{10}$. The adsorption mechanism of hydrogen adsorption on substrates is discussed using energetic diagram in the HOMO-LUMO region.

2. Method

Figure 1 shows the two pyrene-like clusters. The interactions of hydrogen with $C_{16}H_{10}$ and $B_8N_8H_{10}$ were determined variationally in the framework of hybrid DFT. The calculations were carried out using the GAUSSIAN 98 software package [19]. The basis set used in the present study is Pople's 6-31G(d). For the exchange-correlation density functional, we used the combination of Becke's three-parameter exchange functional with Lee, Yang, and Parr's correlation functional (B3LYP) [20,21]. Spin polarization of the electron is allowed by means of the unrestricted Kohn-Sham approach. We performed structure optmization and potential energy surface analysis with respect to the adsorbate-substrate distance. For the potential energy surface calculation, relaxation approach is employed, where the relaxed structures of H-$C_{16}H_{10}$ and H-$B_8N_8H_{10}$ have been calculated with the fixed distance between hydrogen and the substrates. The calculation parameters were taken as follows: SCF convergence: 10^{-6} Hartree for single points and for the potential energy surface (PES).

---

* Corresponding author. Tel: +81-72-751-9523; fax: +81-72-751-9637; E-mail: k.ohta@aist.go.jp

doi:10.1016/j.synthmet.2005.07.331

Geometry optimization: displacement at 10^{-3} Bohr, gradient at 10^{-3} Hartree/Bohr, and energy at 10^{-5} Hartree.

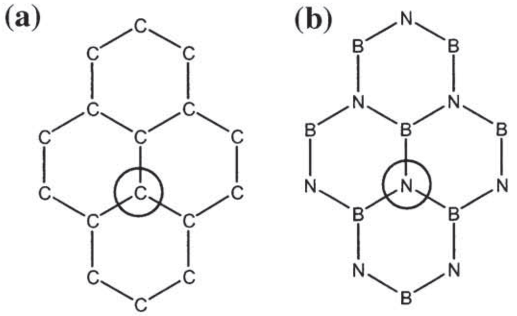

Fig. 1. The skeletal structures of substrates. Drawing hydrogen atoms is omitted. The circled atoms mean the adsorbent atoms.
(a) $C_{16}H_{10}$; (b) $B_8N_8H_{10}$.

4. Results and discussion

Figure 2 shows the potential energy curve as a function of the adsorbate-substrate distance. The global minimum point is located on 1.121 Å for H-$C_{16}H_{10}$ and 3.450 Å for H-$B_8N_8H_{10}$. The dissociation energies of H-$C_{16}H_{10}$ and H-$B_8N_8H_{10}$ are 53.8 and 0.61 kJ/mol, respectively. Comparing the H-$C_{16}H_{10}$ and H-$B_8N_8H_{10}$ potential energy curves, it can be seen that there is large difference in the well depth around 1.1 Å. For the H-$C_{16}H_{10}$ potential energy curve, there is a stable chemisorption region, while for the H-$B_8N_8H_{10}$ case it is a metastable region. The well depth of H-$B_8N_8H_{10}$ is quite shallow compared to that of H-$C_{16}H_{10}$.

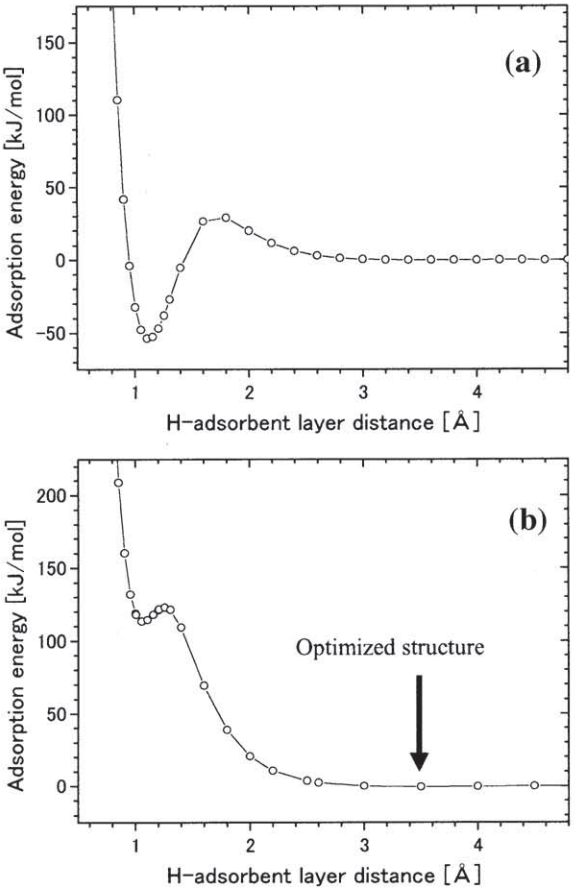

Fig. 2. Potential energy curve as a function of adsorbate-substrate distance. (a) H-$C_{16}H_{10}$. (b) H-$B_8N_8H_{10}$.

Figure 3(a) shows the optimized structures of H-$C_{16}H_{10}$. It can be seen that the $C_{16}H_{10}$ substrate significantly deviates from the planar structure. In particular, the deformation around the substrate C atom is pronounced. The electron densities of adsorbate H and adsorbent C of H-$C_{16}H_{10}$ are 0.26 and -0.34, respectively. This clear charge transfer shows that the C-H binding has chemical nature.

Figure 3(b) shows the optimized structure of H-$B_8N_8H_{10}$. The $B_8N_8H_{10}$ substrate keeps a planar structure, implying weak interaction of H with $B_8N_8H_{10}$. The electron densities of adsorbate H and adsorbent N of H-$B_8N_8H_{10}$ are 0.002 and -0.44, respectively. This small charge transfer means that the H-N binding is much closer to the physisorption type. This is consistent with the small dissociation energy, 0.61 kJ/mol.

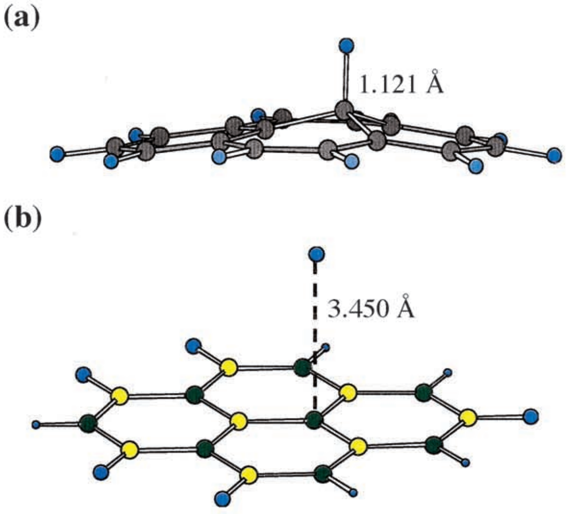

Fig. 3. Optimized structures. (a) H-$C_{16}H_{10}$. Blue and gray circles represent the hydrogen and carbon atoms, respectively. (b) H-$B_8N_8H_{10}$. Blue, yellow, and green circles represent hydrogen, boron, and nitrogen atoms, respectively.

In order to understand the difference in the binding strength of H to substrates under study, we show in Fig. 4 the energetic diagram in the HOMO-LUMO region for $C_{16}H_{10}$, H-$C_{16}H_{10}$, $B_8N_8H_{10}$, and H-$B_8N_8H_{10}$.

The $C_{16}H_{10}$ and $B_8N_8H_{10}$ clusters were studied in those optimized geometries, and H-$C_{16}H_{10}$ and H-$B_8N_8H_{10}$ were in those relaxed geometries with fixed adsorbate-substrate distances of 3.45 Å. For H-$B_8N_8H_{10}$, it means the global minimum structure. On the whole, the patterns of the MO phase of $C_{16}H_{10}$ and H-$C_{16}H_{10}$ are similar to those of $B_8N_8H_{10}$ and H-$B_8N_8H_{10}$, respectively.